Formation of iodinated products in Fe (II)/peroxydisulfate (PDS) system

Zijun Dong, Mu Li, Meifen Chen, Yurong Gu, Chengchun Jiang and Feiyun Sun

ABSTRACT

The transformation of iodide (I^-) and hypoiodous acid (IO^-) by Fe (II)-activated peroxydisulfate (PDS) in the presence of natural organic matter (NOM) was investigated. In the water of a reservoir in Shenzhen, four kinds of organic matter were detected: iodoform > diiodo-bromomethane > dibromo-iodomethane > dichloromethane. As pH increased from 3 to 10, I^- conversion rate decreased from 31.0% to 11.0%. There is basically no iodic acid (IO_3^-) generated under alkaline conditions, probably due to these organic matters. When PDS concentration is low, PDS can oxidize part of I^- to IO^-, and the oxidation of I^- into IO_3^- reaction and continued oxidation reaction exist at the same time, so some IO_3^- is generated in the system. As the proportion of Fe (II) increases, the generation rate of IO_3^- gradually increases. When Fe^{2+}/PDS is 1:5, 2:5, and 3:5, the conversion rates of IO_3^- are 4.7%, 6.5%, and 8.4%, respectively. There are two main reasons for this: (i) the reaction of IO^- produced in the system with humic acid (HA) inhibits the further conversion of IO^- to IO_3^-; (ii) both HA and I- in the system can react with PDS, resulting in a reduction in the oxidation rate of I^-.

Key words | Fe (II), iodide, natural organic matter (NOM), peroxydisulfate (PDS)

Zijun Dong
Meifen Chen
Yurong Gu (corresponding author)
Chengchun Jiang
School of Civil and Environmental Engineering,
Shenzhen Polytechnic,
Shenzhen 518055,
China
E-mail: *gyr0809405018@szpt.edu.cn*

Mu Li
Shenzhen Environmental Science and New Energy Laboratory, Tsinghua-Berkeley Shenzhen Institute,
Tsinghua University,
Shenzhen,
China

Feiyun Sun
School of Civil and Environmental Engineering,
Harbin Institute of Technology (Shenzhen),
Shenzhen 518055,
China

HIGHLIGHTS

- Formation of I-DBPs by Fe (II)/PDS process in real water was evaluated.
- I-DBPs generation in various reaction conditions was examined.
- Existence of HA showed apparent inhibition on IO_3^- generation.

doi: 10.2166/ws.2020.254

GRAPHICAL ABSTRACT

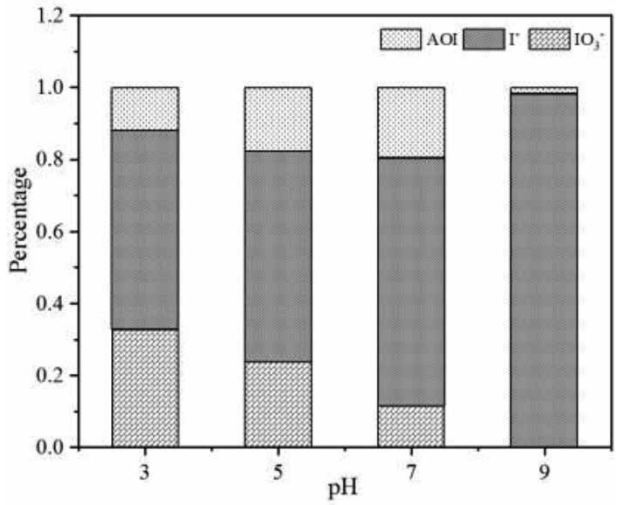

INTRODUCTION

In the natural water environment, the main forms of iodide are iodide ions (I^-) and iodic acid (IO_3^-) (Bichsel & Von Gunten 1999; Richardson *et al.* 2008; Zhao *et al.* 2016). In addition to iodine in natural water, iodine enters water in industrial and medical industries, such as iodinated X-ray contrast media (ICM compounds), causing serious iodine pollution (Pérez & Barceló 2007; Duirk *et al.* 2011). Iodide readily reacts with oxidants to form hypoiodous acid (HOI) such as permanganate ($KMnO_4$), ozone (O_3), UV (Magi *et al.* 1997; Criquet *et al.* 2012; De la Cruz *et al.* 2012; Yang *et al.* 2014). During oxidation, two pathways are conducted: (i) HOI reacts with natural organic matter (NOM) in water to produce a series of iodine by-products (I-DBPs), including IO_3^- and iodomethane, (ii) HOI is further oxidized to iodate (IO_3^-) (Li *et al.* 2017; Dong *et al.* 2019). During the past decade, it has been investigated that I-DBPs are more toxic than chlorinated and brominated by-products, so there is an urgent need for a way to control iodine by-products in water bodies (Smith *et al.* 2010; Gan *et al.* 2015; Liu *et al.* 2017; Hu *et al.* 2018; Huang *et al.* 2019). The generation factors of I-DBPs are affected by the quality of the raw water, the type of oxidant, the pH of the water and the concentration of I– in the water (Tian *et al.* 2014; Dong *et al.* 2018; Hu *et al.* 2019; Wu *et al.* 2019; Zhao *et al.* 2019). The NOM in the water body reacts with the oxidant to produce by-product precursors. The properties of these precursors have a certain influence on the production of iodine by-products (Dong *et al.* 2019). The types of precursor organic matter directly affect the types of by-products. The oxidant can sequentially oxidize the I^- to IO^- and IO_3^- (Li *et al.* 2017). The IO_3^- will not react with organic matter to form iodine by-products, and the reaction rates of hypoiodine with different oxidants are different. Previous studies have investigated that peroxymonosulfate was able to oxidize I^-, the second-order rate constant of reaction was $1.01 \times 10^3\ M^{-1}\ s^{-1}$, while that for HOI was $1.08 \times 10^2\ M^{-1}\ s^{-1}$ (Li *et al.* 2017). Studies have shown that the concentration of iodized trihalomethanes increased with the concentration of I^- in raw water (Hua *et al.* 2006; Allard *et al.* 2016; Kralchevska *et al.* 2016; Liu *et al.* 2017).

Among all oxidants, $SO_4^{\cdot-}$ is a highly active oxidant with unsaturated electronic structure and unstable chemical properties, which has the characteristics of strong oxidation and short half-life. Under neutral conditions, the oxidation–reduction potential of $SO_4^{\cdot-}$ is higher than $^{\cdot}OH$, and most organic pollutants can be completely degraded by $SO_4^{\cdot-}$ (Anipsitakis & Dionysiou 2003). The transformation of pollutants by $SO_4^{\cdot-}$ usually follows three pathways: (i) $SO_4^{\cdot-}$

degrades saturated organics such as alkanes, alcohols, and lipids through hydrogen atom extraction; (ii) $SO_4^{\cdot-}$ passes through unsaturated bonds of unsaturated olefins by addition reaction (House 1962; Rastogi *et al.* 2009; Wu *et al.* 2012; Ding *et al.* 2013; Xie *et al.* 2015); (iii) electron transfer reaction. However, there is little information about I^- conversion in the $SO_4^{\cdot-}$ system oxidation process. The result of rapid conversion of I^- to HOI by $SO_4^{\cdot-}$ indicates that the potential genotoxicity and cytotoxicity of I-DBP are usually several to hundreds of times higher than its chlorinated and brominated analogs. Peroxydisulfate (PDS), as an oxidant that is relatively stable at room temperature, has strong oxidizing properties and high solubility, and it has gradually been used in the environmental field (House 1962; Wu *et al.* 2012). The advantages enable PDS to be used in new types of advanced oxidation technologies. Thermal activation, ultraviolet activation, metal ion and metal oxide activation methods are the most common activation methods reported in the literature. Transitional metal can activate PDS to produce $SO_4^{\cdot-}$ with the activation energy required for metal ion catalysis being low, about 50 kJ/mol (Zhao *et al.* 2019). However, in the Fe^{2+}/PDS system, due to the complexity of NOMs in the water, the types of I-DBPs generated are also more complex, transforming with the variation of environment (Kamarehie *et al.* 2017; Mohagheghian *et al.* 2017). The objectives of this study were (i) to investigate the varieties of I-DBPs in a natural water environment and (ii) to explore the generation of I-DBPs in the Fe (II)/PDS oxidation process under different factors.

MATERIALS AND METHODS

Chemicals

Sodium persulfate (PDS) with purity 99%, NaClO (6%–14% active chlorine), KI with purity >99% and KIO_3 with purity 99.8% were purchased from Shanghai Aladdin. Ferrous sulfate with purity >99%, ferric sulfate with purity 97%, nitrobenzene with purity >99%, sodium hydroxide with purity >96%, and sulfuric acid (purity 95%–98%) were purchased from Sinopharm Chemical Reagent Co. Ltd. Methanol, acetonitrile and acetic acid with purity >99% were purchased from Merck. All solutions were prepared using deionized water with 18.2 MΩ/cm Milli-Q water.

Formation of iodinated products

All the experiments were conducted in a 250 mL batch reactor at temperature 25 °C. Add a pre-configured buffer solution containing 4 mM sodium tetraborate/potassium dihydrogen phosphate to a 250 mL iodine flask, add a calculated volume of KI standard solution, and prepare the concentration of KI required for the experiment. Use 0.1 mol/L H_2SO_4 or 0.1 mol/L NaOH to adjust the pH of the prepared KI solution to the set value. The sampling amount is determined according to the amount of target substance required to determine the index, and a certain volume of sodium sulfite needs to be added immediately after sampling to terminate the reaction. After the end, the pH change is less than 0.2.

When measuring IO_3^-, add a calculated volume of Fe (II) to a 250 mL iodine flask, then add a calculated volume of PDS, and at the same time start timing sampling, take 1 mL and add it to the liquid phase containing 2,6-dichlorophenol and anhydrous sodium sulfite. In a vial, measure hypoiodic acid, take 5 mL and add it to an ion chromatography tube containing anhydrous sodium sulfite, and measure iodide ion and hypoiodic acid. In order to ensure the reliability of the experimental results, each group of experiments was repeated three times, and the error of the experimental results was controlled within 5%, and a blank experiment was set.

Analysis

I^-, IO^- and IO_3^-

I^-, IO_3^- and IO^- were measured by ion chromatography (ICS1500). The specific chromatographic conditions are a Dionex ICS1500 ion chromatograph (USA); isocratic leaching is used, the eluent is 9 mmol/L Na_2CO_3; the flow rate of the eluent is 1 mL/min; the suppression method is conductivity suppression, which is caused by electrolytic water producing H^+, the suppressor is an ASRS-Ultra 2 mm external water anion suppressor; column temperature: 35 °C; the detector is a conductivity detector; detector temperature is

35 °C; chromatographic column: IonpacAS9 type protection column (4 mm × 4 mm); IonPacAS9-HC type separation column (250 mm × 4 mm); injection volume is 1,000 μg/L; method detection limit is 0.3 μg/L. The detection of IO^- used the method of reacting IO^- with 2,6-dichlorophenol to produce 4-iodo-2,6-dichlorophenol, by measuring the amount of 4-iodo-2,6-dichlorophenol. The 4-iodo-2,6-dichlorophenol was measured by Waters high performance liquid chromatography under the conditions of: C18 column (4.6 mm × 250 mm × 5 μm), and the mobile phase is V(acetonitrile): V(water) = 7:3, ultraviolet detection wavelength is 212 nm, flow rate is 1 mL/min, injection volume is 100 uL.

Formation of I-DBPs in water

The determination of I-DBPs is carried out by combined use of gas and quality. Gas chromatographic conditions: HP-5MS capillary column (30.0 m × 0.25 mm × 0.25 μm), electron capture detector, detector temperature is 300 °C, inlet temperature is 200 °C, program temperature is 40 °C, hold for 5 min, to raise 1 °C/min to 45 °C, hold for 3 min, raise 10 °C/min to 135 °C, then raise 25 °C/min to 220 °C, inject 1 μL, splitless injection. Mass spectrometry conditions: EI ion source, ion source temperature 225 °C, quadrupole temperature 150 °C, chromatography–mass spectrometer connection temperature 170 °C, electron energy 70 eV, solvent delay 3 min, scan mass range m/z 20–500, scan mode select ion monitoring (m/z).

Extraction conditions by gas mass spectrometry: MTBE is used as the extractant. At the end of the reaction, a 30 mL sample and a bottle with a Teflon cap are taken, 6 g of anhydrous sodium carbonate is added to shake, and a 3 mL pure MTBE solution is added to the sample with a pipette gun. In the test, shake for 20 minutes in a vortex shaker and stand still for 20 minutes. Take 1 mL of the upper layer organic solution in the sample bottle with the air quality for detection.

AOI

Absorbable organic halogen (AOI) was measured with a Multi X 2500 total organic halogen analyzer (Analytic Jena, Germany). An APU28 carbon column was used for sample adsorption. Add nitric acid stock solution to the sample, the pH value of the whole sample is less than 2, take a 50 mL sample in the pressure filter, and set the program. After the sample passes through the APU28, the AOI in it is completely adsorbed on the APU28 carbon column. Then elute the ions in the carbon column with 25 mL sodium nitrate stock solution, take out the sample carbon column at the end of the desorption, and absorb the surface moisture on the filter paper; put the sample carbon column into the combustion tube, mineralize at 950 °C, AOI is converted into HI gas; HI gas is dehydrated by concentrated sulfuric acid, and detected by high-sensitivity microcoulometric titration. In order to ensure reliable measurement results, 2-iodophenol is used as the standard substance for calibration.

RESULTS AND DISCUSSION

Formation of I-DBPs in real water

The formation of I-DBPs is closely related to the type of organic matter in the water. In the actual water body, the organic matter contained in it is relatively complex, including multiple functional groups: benzene rings, amino groups, carboxyl groups, etc. The type of organic matter may be different from the products formed by PDS oxidation, but the possible paths and mechanisms for functional groups are similar. To investigate I-DBPs formation during oxidation of PDS by Fe (II) in real water, I^- was spiked into the river water from a reservoir from Shenzhen. Six typical iodinated organic compounds (bromochloroiodomethane, monobromodiiodomethane, dibromomonoiodomethane, monochlorodiiodomethane, dichloromonoiodomethane, iodoform) were monitored.

Figure 1 shows the determination of I-DBPs at an initial PDS concentration 100 μM, Fe (II) concentration 80 μM and pH 3, over 120 min. The results suggest that the concentration order of the detected four kinds of organic matter is: iodoform > diiodo-bromomethane > dibromo-iodomethane > dichloromethane, the maximum concentration of iodoform is 0.49 μM, and the concentration of iodoform can induce cell mutagenesis and endanger human health. In addition to the detected iodine by-products, there are also iodine by-products including

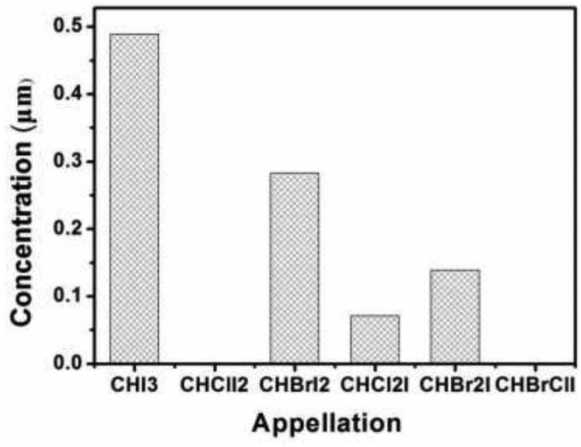

Figure 1 | Determination of iodomethane in actual water (pH = 3, [Fe (II)] = 80 μM, $T = 25$ °C, $t = 120$ min).

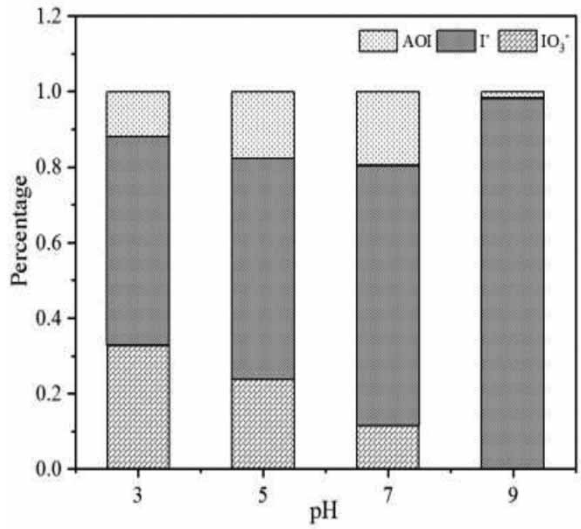

Figure 2 | Effect of pH on the formation of I^- transformation ([PDS] = 100 μM, [I^-] = 10 μM, [Fe^{2+}/PDS] = 4:5, [HA] = 5 mg/L, $T = 25$ °C).

diiodine-bromomethane, iodine dichloromethane, and iodine dibromomethane in the water, all of which are highly toxic. Due to the instability of the actual water body, all the iodine-containing organic substances are characterized by an index of the sum of iodine by-products in the experiment – Adsorbable Organic Iodine (AOI).

Effect of initial pH

The oxidation effect of PDS at different pH is different. At the same time, pH also affects the type of active iodine produced by PDS oxidizing iodine ions, and the type of active iodine is greatly different in the degree of difficulty of being reacted by the oxidant. The pH affects the ability of PDS to oxidize I^-, the presence of Fe (II) in the experimental system, and the rate of PDS oxidation of active iodine. Therefore, the types and amounts of I-DBPs produced under different pH conditions will be quite different.

The change of formation of I^- transformation with pH in the Fe (II)/PDS system is illustrated in Figure 2. The ratio of the Fe (II) transformation to PDS was 4:5 as pH was increased from 3 to 10. As the pH increases, the total amount of AOI gradually increases and then slowly decreases, IO_3^- gradually decreases as the pH increases, I^- gradually increase as the pH increases and the concentration of IO^- is barely detectable in the solution. For IO_3^-, 31% of the I^- are converted to IO_3^- at pH 3. While in organic-free systems, the IO_3^- generation rate is 56% and gradually decreases at pH = 4, 5, 6, and 7. Especially, there is basically no IO_3^- generated under alkaline conditions, probably due to the organic matter. When the system generates IO_3^-, it is quickly captured and cannot be oxidized. For I^-, the conversion efficiency of I^- gradually decreases with increasing pH. As the pH increases from 3 to 9, the remaining amount of I^- rises from 57% to 98%. Compared with the absence of organic matter, the conversion efficiency of I^- is also greatly reduced at the same pH. This is because the organic substances in the system react with sulfate radicals generated by Fe (II)/PDS, and the free radicals participating in the oxidation reaction of I^- decrease, so that the conversion rate of I^- decreases. No IO^- was detected in the system with organic matter. This is because a large amount of organic matter causes a part of the IO^- produced by the reaction to be captured and a part of it to be oxidized to IO_3^-. It can be seen from the iodine conservation curve that the total iodine amount of I^- plus IO_3^- plus AOI is close to the total amount of iodine, basically reaching iodine conservation.

Effect of initial PDS dosage

Figure 3 shows the effect of PDS dosage on the I^- transformation in the Fe (II)/PDS system, at a constant Fe (II) dosage

of 20 μM, and I^- initial concentration of 10 μM. The ratio of the Fe (II) transformation to PDS was 4:5 at pH 3. When the concentration of the PDS is low, PDS can oxidize part of I^- to IO^-, and the oxidation of I^- into IO_3^- reaction and the continued oxidation reaction exist at the same time, so some IO_3^- is generated in the system. However, due to the limited concentration of PDS, IO^- that has not been oxidized to IO_3^- can quickly react with organic matter to form I-DBPs. The concentration of IO_3^- increases with the increase of the PDS concentration, and it stabilizes at 100 μM, indicating that the higher the PDS concentration, the more thorough the oxidation reaction that occurs, and the higher the I conversion rate, the saturation reaches 100 μM. For I^-, the higher the PDS concentration, the lower the iodine ion concentration, indicating that more I^- are oxidized. The sum of I^- and IO_3^- concentration after 40 μM is almost unchanged, indicating that the PDS concentration has a greater influence on the first step of the iodine oxidation reaction, and has little effect on the conversion of IO^- to I-DBPs. The law of AOI decreases with the increase of oxidant concentration, which is the largest at 60, indicating that under this condition, secondary iodine easily reacts with organic matter to form iodine byproducts.

Effect of initial Fe (II)/PDS molar ratio

Figure 4 shows the effect of Fe (II)/PDS on I^- transformation in the Fe (II)/PDS system, at a constant PDS dosage of 100 μM, I^- initial concentration of 10 μM at pH 3. As the proportion of Fe (II) increases, the generation rate of IO_3^- gradually increases. When Fe^{2+}/PDS is 1:5, 2:5, and 3:5, the conversion rates of IO_3^- are 4.7%, 6.5%, and 8.4, respectively. When Fe^{2+}/PDS reaches 5:5, about 33% of I^- are oxidized to IO_3^-. When Fe^{2+}/PDS reaches 6:5, 36% of the I^- are converted to IO_3^-, indicating that at Fe^{2+}/PDS ratio greater than 4:5, a large amount of I^- are converted into IO^- in the experimental system, and then further converted into IO_3^-, and when Fe^{2+}/PDS is small, the activation generates fewer sulfate radicals and the ability to oxidize I^- is insufficient, so the generation rate of IO_3^- is small.

The conversion rate of I^- is similar to that of IO_3^-. It gradually increases with the increase of Fe^{2+}/PDS, and then tends to be stable. It can be seen from the figure that when Fe^{2+}/PDS is 6:5, the residual amount of iodide ion is the smallest at 48%, and the conversion rate is the largest. When the Fe^{2+}/PDS ratio is 1:5, the residual amount of iodide ion reaches 73%.

The AOI in the experimental system gradually increases with the increase of the proportion of ferrous iron and then decreases. When the Fe^{2+}/PDS ratio is 3:5, the AOI generation rate is 30% at the maximum, and the Fe^{2+}/PDS ratio

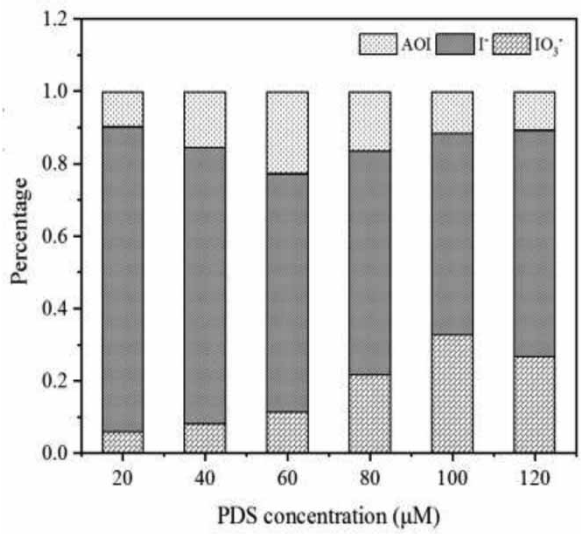

Figure 3 | Effect of PDS dosage on the formation of I^- transformation (pH 3, $[I^-] = 10$ μM, $[Fe^{2+}/PDS] = 4:5$, [HA] = 5 mg/L, $T = 25$ °C).

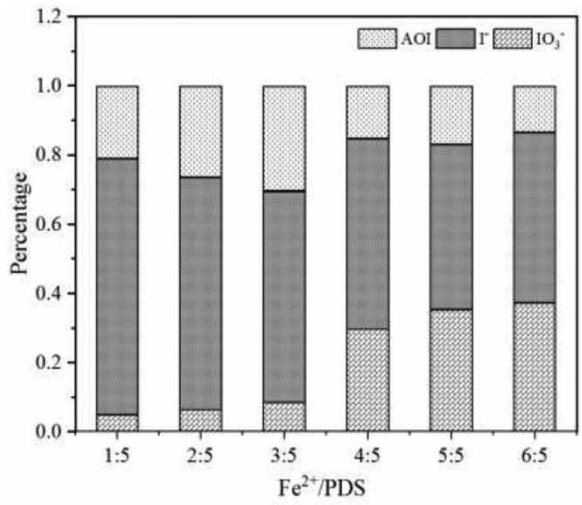

Figure 4 | Effect of Fe (II)/PDS on the formation of I^- transformation (pH 3, [PDS] = 100 μM, $[I^-] = 10$ μM, [HA] = 5 mg/L, $T = 25$ °C).

is 4:5, 5:5 and 6:5. The generation rates of AOI are 15.9%, 15.7% and 14.0%.

Effect of NOM

The effect of NOM on I^- transformation in the Fe(II)/PDS system was examined in the presence of commercial humic acid (HA; used as a representative NOM), at pH 3. As can be seen in Figure 5, as the concentration of HA increases, the AOI in the system gradually increases. When the HA concentration reaches 1 mg/L, the AOI reaches the maximum. When the HA concentration in the experimental system is increased again, AOI concentration remains basically unchanged. The amount of IO_3^- produced gradually decreases with increasing HA concentration. There are two main reasons for this: (i) the reaction of IO^- produced in the system with HA inhibits the further conversion of IO^- to IO_3^-; (ii) both HA and I^- in the system can react with PDS, resulting in a reduction in the oxidation rate of I^-.

From this we can conclude that the total organic carbon of the water body affects the generation of I-DBPs in the water. It is not that the higher the TOC, the easier it is for the water body to produce I-DBPs. We can also control I-DBPs by controlling the total organic carbon product formation.

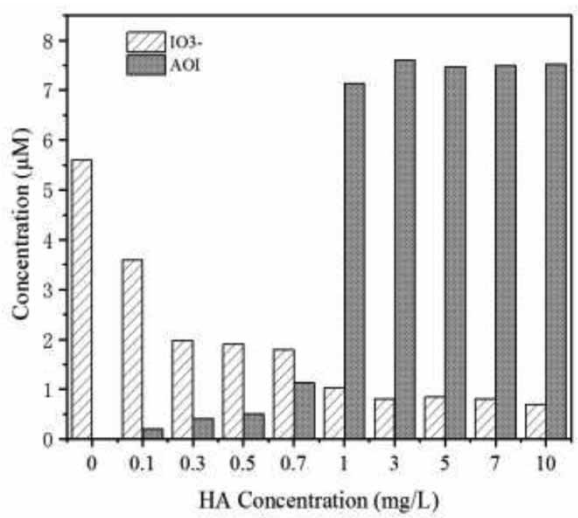

Figure 5 | Effect of HA on the formation of I^- transformation (pH 3, [PDS] = 100 μM, [I^-] = 10 μM, [Fe^{2+}/PDS] = 4:5, T = 25 °C).

CONCLUSIONS

This study investigated the Fe (II) activated PDS process under different pH, Fe (II)/PDS, PDS dosage and NOM conditions. Based on the experimental results obtained, the following conclusions can be obtained:

(1) The experiment results verified the generation of AOI in the case of adding NOM to the Fe (II)/PDS oxidation system. It was found that under acidic conditions, as the AOI formation rate is larger, I^- production is more.
(2) Under alkaline conditions, although the AOI generation rate is small, the conversion rate of iodide ions is small. When the concentration of oxidant in the experimental system is increased, the AOI generation amount gradually increases and then decreases.
(3) The AOI generation increases with the proportion of Fe (II). When the ratio is 3:5, the generation rate of AOI is at most 30%. The generation of AOI gradually increases with the increase of HA concentration, and when the concentration is 1 mg/L, the AOI concentration is the largest.

ACKNOWLEDGEMENT

We thank funding support from Guangdong Basic and Applied Basic Research Foundation (Grant No. 2020A1515011545), Shenzhen Water Group Program (Grant No. 2019-131-F) and Shenzhen Polytechnic Program (Grant No. 6019310013K0).

DATA AVAILABILITY STATEMENT

All relevant data are included in the paper or its Supplementary Information.

REFERENCES

Allard, S., Criquet, J., Prunier, A., Falantin, C., Le Person, A., Tang, J. Y.-M. & Croué, J.-P. 2016 Photodecomposition of iodinated contrast media and subsequent formation of toxic iodinated

moieties during final disinfection with chlorinated oxidants. *Water Research* **103**, 453–461.

Anipsitakis, G. P. & Dionysiou, D. D. 2003 Degradation of organic contaminants in water with sulfate radicals generated by the conjunction of peroxymonosulfate with cobalt. *Environmental Science & Technology* **37** (20), 4790–4797.

Bichsel, Y. & von Gunten, U. 1999 Oxidation of iodide and hypoiodous acid in the disinfection of natural waters. *Environmental Science & Technology* **33** (22), 4040–4045.

Criquet, J., Allard, S., Salhi, E., Joll, C. A., Heitz, A. & von Gunten, U. 2012 Iodate and iodo-trihalomethane formation during chlorination of iodide-containing waters: role of bromide. *Environmental Science & Technology* **46** (13), 7350–7357.

De la Cruz, N., Giménez, J., Esplugas, S., Grandjean, D., de Alencastro, L. F. & Pulgarín, C. 2012 Degradation of 32 emergent contaminants by UV and neutral photo-fenton in domestic wastewater effluent previously treated by activated sludge. *Water Research* **46** (6), 1947–1957.

Ding, Y., Zhu, L., Wang, N. & Tang, H. 2013 Sulfate radicals induced degradation of tetrabromobisphenol A with nanoscaled magnetic $CuFe_2O_4$ as a heterogeneous catalyst of peroxymonosulfate. *Applied Catalysis B: Environmental* **129**, 153–162.

Dong, H., Qiang, Z., Liu, S., Li, J., Yu, J. & Qu, J. 2018 Oxidation of iopamidol with ferrate (Fe(VI)): kinetics and formation of toxic iodinated disinfection by-products. *Water Research* **130**, 200–207.

Dong, Z., Jiang, C., Yang, J., Zhang, X., Dai, W. & Cai, P. 2019 Transformation of iodide by Fe(II) activated peroxydisulfate. *Journal of Hazardous Materials* **373**, 519–526.

Duirk, S. E., Lindell, C., Cornelison, C. C., Kormos, J., Ternes, T. A., Attene-Ramos, M., Osiol, J., Wagner, E. D., Plewa, M. J. & Richardson, S. D. 2011 Formation of toxic iodinated disinfection by-products from compounds used in medical imaging. *Environmental Science & Technology* **45** (16), 6845–6854.

Gan, W., Sharma, V. K., Zhang, X., Yang, L. & Yang, X. 2015 Investigation of disinfection byproducts formation in ferrate(VI) pre-oxidation of NOM and its model compounds followed by chlorination. *Journal of Hazardous Materials* **292**, 197–204.

House, D. A. 1962 Kinetics and mechanism of oxidations by peroxydisulfate. *Chemical Reviews* **62** (3), 185–203.

Hu, S., Gong, T., Xian, Q., Wang, J., Ma, J., Li, Z., Yin, J., Zhang, B. & Xu, B. 2018 Formation of iodinated trihalomethanes and haloacetic acids from aromatic iodinated disinfection byproducts during chloramination. *Water Research* **147**, 254–263.

Hu, J., Wang, C., Ye, Z., Dong, H., Li, M., Chen, J. & Qiang, Z. 2019 Degradation of iodinated disinfection byproducts by VUV/UV process based on a mini-fluidic VUV/UV photoreaction system. *Water Research* **158**, 417–423.

Hua, G., Reckhow, D. A. & Kim, J. 2006 Effect of bromide and iodide ions on the formation and speciation of disinfection byproducts during chlorination. *Environmental Science & Technology* **40** (9), 3050–3056.

Huang, Y., Zhang, Y., Zhou, Q., Li, A., Shi, P., Qiu, J. & Pan, Y. 2019 Detection, identification and control of polar iodinated disinfection byproducts in chlor(am)inated secondary wastewater effluents. *Environmental Science: Water Research & Technology* **5** (2), 397–405.

Kamarehie, B., Mohamadian, J., Mousavi, S. A., Asgari, G. & Shahamat, Y. D. 2017 Aniline degradation from aqueous solution using electro/Fe^{2+}/peroxydisulphate process. *Desalination and Water Treatment* **80**, 337–343.

Kralchevska, R. P., Sharma, V. K., Machala, L. & Zboril, R. 2016 Ferrates (Fe^{VI}, Fe^{V}, and Fe^{IV}) oxidation of iodide: formation of triiodide. *Chemosphere* **144**, 1156–1161.

Li, J., Jiang, J., Zhou, Y., Pang, S.-Y., Gao, Y., Jiang, C., Ma, J., Jin, Y., Yang, Y., Liu, G., Wang, L. & Guan, C. 2017 Kinetics of oxidation of iodide (I^-) and hypoiodous acid (HOI) by peroxymonosulfate (PMS) and formation of iodinated products in the PMS/I^-/NOM system. *Environmental Science & Technology Letters* **4** (2), 76–82.

Liu, S., Li, Z., Dong, H., Goodman, B. A. & Qiang, Z. 2017 Formation of iodo-trihalomethanes, iodo-acetic acids, and iodo-acetamides during chloramination of iodide-containing waters: factors influencing formation and reaction pathways. *Journal of Hazardous Materials* **321**, 28–36.

Magi, L., Schweitzer, F., Pallares, C., Cherif, S., Mirabel, P. & George, C. 1997 Investigation of the uptake rate of ozone and methyl hydroperoxide by water surfaces. *The Journal of Physical Chemistry A* **101** (27), 4943–4949.

Mohagheghian, A., Naghipour, D., Moslemzadeh, M. & Taghavi, K. 2017 Photochemical degradation of 2,4-dichlorophenol in aqueous solutions by Fe^{2+}/peroxydisulfate/UV process. *International Journal of Engineering* **30** (1), 15–22.

Pérez, S. & Barceló, D. 2007 Fate and occurrence of X-ray contrast media in the environment. *Analytical and Bioanalytical Chemistry* **387** (4), 1235–1246.

Rastogi, A., Al-Abed, S. R. & Dionysiou, D. D. 2009 Sulfate radical-based ferrous–peroxymonosulfate oxidative system for PCBs degradation in aqueous and sediment systems. *Applied Catalysis B: Environmental* **85** (3–4), 171–179.

Richardson, S. D., Fasano, F., Ellington, J. J., Crumley, F. G., Buettner, K. M., Evans, J. J., Blount, B. C., Silva, L. K., Waite, T. J., Luther, G. W., McKague, A. B., Miltner, R. J., Wagner, E. D. & Plewa, M. J. 2008 Occurrence and mammalian cell toxicity of iodinated disinfection byproducts in drinking water. *Environmental Science & Technology* **42** (22), 8330–8338.

Smith, E. M., Plewa, M. J., Lindell, C. L., Richardson, S. D. & Mitch, W. A. 2010 Comparison of byproduct formation in waters treated with chlorine and iodine: relevance to point-of-use treatment. *Environmental Science & Technology* **44** (22), 8446–8452.

Tian, F.-X., Xu, B., Lin, Y.-L., Hu, C.-Y., Zhang, T.-Y. & Gao, N.-Y. 2014 Photodegradation kinetics of iopamidol by UV irradiation and enhanced formation of iodinated disinfection

by-products in sequential oxidation processes. *Water Research* **58**, 198–208.

Wu, J., Zhang, H. & Qiu, J. 2012 Degradation of Acid Orange 7 in aqueous solution by a novel electro/Fe^{2+}/peroxydisulfate process. *Journal of Hazardous Materials* **215–216**, 138–145.

Wu, Y., Zhu, S., Zhang, W., Bu, L. & Zhou, S. 2019 Comparison of diatrizoate degradation by UV/chlorine and UV/chloramine processes: kinetic mechanisms and iodinated disinfection byproducts formation. *Chemical Engineering Journal* **375**, 121972.

Xie, P., Ma, J., Liu, W., Zou, J., Yue, S., Li, X., Wiesner, M. R. & Fang, J. 2015 Removal of 2-MIB and geosmin using UV/persulfate: contributions of hydroxyl and sulfate radicals. *Water Research* **69**, 223–233.

Yang, Y., Komaki, Y., Kimura, S. Y., Hu, H.-Y., Wagner, E. D., Mariñas, B. J. & Plewa, M. J. 2014 Toxic impact of bromide and iodide on drinking water disinfected with chlorine or chloramines. *Environmental Science & Technology* **48** (20), 12362–12369.

Zhao, X., Salhi, E., Liu, H., Ma, J. & von Gunten, U. 2016 Kinetic and mechanistic aspects of the reactions of iodide and hypoiodous acid with permanganate: oxidation and disproportionation. *Environmental Science & Technology* **50** (8), 4358–4365.

Zhao, X., Jiang, J., Pang, S., Guan, C., Li, J., Wang, Z., Ma, J. & Luo, C. 2019 Degradation of iopamidol by three UV-based oxidation processes: kinetics, pathways, and formation of iodinated disinfection byproducts. *Chemosphere* **221**, 270–277.

First received 24 July 2020; accepted in revised form 22 September 2020. Available online 16 October 2020